Hydrogen-Bonding Interactions in Gas-Phase Polyether / Ammonium Ion Complexes

C.-C. Liou, H.-F. Wu, and J.S. Brodbelt
Department of Chemistry and Biochemistry, University of Texas, Austin, Texas, USA

Hydrogen bonds are among the most important interactions involved in selective complexation in host–guest chemistry. In this study a variety of hydrogen-bonded crown ether/ammonium ion complexes are generated in the gas phase by association reactions between an amine substrate and a polyether, one of which is initially protonated, and stabilized by many collisions in the chemical ionization source of a triple quadrupole mass spectrometer or in a quadrupole ion trap. The nature of the hydrogen-bonding interactions of the ion complexes are evaluated by comparison of their collision-activated dissociation spectra. After collisional activation, those complexes that are weakly bound dissociate to form intact protonated polyether molecules and/or ammonium ions by simple cleavages of the hydrogen-bond association interactions. In contrast, those complexes strongly bound by multiple hydrogen bonds dissociate not only to the protonated polyether and/or ammonium ions but also by extensive covalent bond cleavage of the protonated ether skeleton.This latter type of dissociation behavior suggests that the polyether/ammonium ion complexes may be sufficiently strongly bound that surpassing the high barrier to decomposition results in formation of internally excited polyether molecules that may then undergo subsequent fragmentation by skeletal cleavages. Moreover, complexes involving multiple hydrogen bonds may have slower dissociation kinetics, allowing competition from fast dissociation processes that have substantial energy barriers. *(J Am Soc Mass Spectrom 1994, 5, 260–273)*

Intermolecular and intramolecular hydrogen bonds are arguably the most important interactions in molecular self assembly and molecular recognition in solution chemistry [1–4]. The formation of a hydrogen bond involves the interaction of a proton donating group, such as a hydroxyl or amino group, and a proton accepting group, such as any group with an unshared electron pair or a pi-electron orbital [3]. Typical hydrogen-bond enthalpies range from 1 to 10 kcal/mol [3]. The configurations of biological macromolecules, such as proteins [5], carbohydrates [6], and nucleic acids [7], are extensively mediated by multiple hydrogen-bonding interactions, and thus there have been numerous studies of the thermochemical parameters of such bonds [5–7].

Hydrogen-bonding interactions are also significant factors in host–guest chemistry [8–15] and site-selective complexation, such as in antibiotic functions and enzyme catalysis. Much of the fundamental understanding of hydrogen-bonding effects in host–guest chemistry has stemmed from studies of simple macrocylic model systems, especially the crown ethers [16–39]. For example, such techniques as NMR, titration calorimetry, and potentiometry have been used to probe the kinetics and thermodynamics of electrostatic complexation of crown ethers with various atomic and polyatomic guests, such as the alkali metal ions [21–24] and ammonium ions [25, 39]. The phenomenon of multiple binding interactions is especially well modeled by crown ethers, which have several identical oxygen donor sites that participate as hydrogen-bond acceptors. The array of binding sites is responsible for the size-selective complexation that is characteristic of macrocycles.

Hydrogen-bonding interactions are also important in the chemistry of gas-phase ions, in particular protonated molecules and proton-bound complexes [40–45]. One recent study reported that intramolecular hydrogen bonds in protonated polyethers could be as strong as 25 kcal/mol as determined from high pressure mass spectrometric measurements of proton-transfer reactions [44]. The total association energies of various polyether/ammonium ion complexes were determined to be 29 to 46 kcal/mol [45], depending on the number of binding sites of the polyether and the structure of the ammonium ion. In fact, multiple hydrogen bonds could contribute up to an additional 21 kcal/mol of binding energy to an ammonium ion/polyether complex (as compared to a complex with a single binding interaction) [45]. Moreover, it was found that even CH ··· O hydrogen bonds contributed to the stabilization of the complexes [45].

Recently we have undertaken a comprehensive study of host–guest chemistry in the gas phase with a series of crown ethers as model hosts [46–51]. For

Address reprint requests to J.S. Brodbelt, Department of Chemistry and Biochemistry, University of Texas, Austin, TX 78712-1167.

1044–0305/94/$7.00

Revised November 8, 1993
Accepted November 15, 1993

example, intrinsic binding selectivities and orders of relative complexation energies have been derived by application of various mass spectrometric techniques, including collision-activated dissociation (CAD) for structural characterization and the kinetic method [52, 53] for determination of orders of guest ion affinities. These preliminary studies and other recent gas-phase investigations [54–56] have established the foundation for gaining insight into host–guest chemistry from a solvent-free perspective.

In the present work a systematic evaluation of the intermolecular binding forces responsible for the association of crown ethers (hosts) with amines (guests) is presented. The nature of hydrogen-bonding interactions of crown ether/ammonium ion complexes is examined with respect to macrocyclic size effects, the gas-phase basicities of 13 different amines, three crown ethers, and nine acyclic ethers, and the number of possible binding interactions. Two types of mass spectrometers, a triple quadrupole instrument equipped with a chemical ionization source and a quadrupole ion trap, were used to obtain complementary information about the nature of the complexes. Low energy CAD is used as a means to assess the relative hydrogen-bonding characteristics of the various polyether/ammonium ion complexes by comparison of the abundances of fragment ions due to covalent bond cleavages of the polyether versus those ions due to simple decomplexation. A summary of the thermochemical and hydrogen-bonding properties of the amine substrates and crown ethers used in this study is shown in Table 1. The gas-phase basicities are shown because they provide a quantitative comparison of the intrinsic ability of each molecule to bind a proton.

Table 1. Thermochemical and structural properties of amines and crown ethers

Substrate	Gas-phase basicity[a] (kcal /mol)	Number of hydrogen-bonding acceptor or donor sites[b]
Ammonia	195.6	4
Propylamine	210.1	3
2,5-Dimethylpyrrole	210.6	1
2-Chloro-6-picoline	211	1
2-Methylaziridine	211.4	2
Pyridine	213.1	1
2-Aminoethanol	213.4	5
3-Aminopropanol	217.3	5
Diethylamine	217.7	2
3,5-Lutidine	217.7	1
Ethylene diamine	219.2	6
4-Aminobutanol	220.7	5
5-Aminopentanol	222	5
12-Crown-4	211.3	4
15-Crown-5	212.5	5
18-Crown-6	216.0	6

[a] From ref 60.
[b] Including all N or O acceptor sites, and all N—H and O—H donor sites.

Experimental

All measurements were performed in a Finnigan triple stage quadrupole mass spectrometer (TSQ-70) equipped with a chemical ionization source or in a Finnigan ion trap mass spectrometer (ITMS) (Finnigan MAT, San Jose, CA). For the experiments in the triple quadrupole instrument, the amines and crown ethers were introduced as a mixture by a direct insertion probe, and typical sample pressure was 1 to 5×10^{-6} torr. Methane was admitted into the source to 2 torr as a protonating chemical ionization agent. Positive ions were formed by using a 70 eV electron beam at 200 μA. The source temperature was 80 °C. Under these conditions the typical relative abundances of product ions formed were $(M_1 + H + M_2)^+$:$(M_n + H)^+ = 2:1$, where M_1 and M_2 represent the polyether and amine introduced into the source. The relatively high pressure of the chemical ionization source ensures that on the average the complexes experience hundreds of collisions, and thus thermal equilibrium conditions are approached. The complexes are most likely formed by gas-phase ion–molecule association reactions between a protonated substrate and a neutral molecule, although complexes could conceivably preform on the solids probe and in some way be volatilized. In these experiments it is impossible to determine whether a protonated amine associates with a neutral crown ether, or whether a protonated crown ether associates with a neutral amine. Both processes yield the ion complex $(M_1 + H + M_2)^+$. The ion complexes were stabilized by numerous deactivating collisions during their residence time prior to collisional activation, and presumably thermochemically favorable configurations were obtained. In the quadrupole ion trap, complexes were formed by allowing a crown ether and ammonia, one of which is initially protonated, to interact in a 50 to 100 ms interval following a 1 ms electron ionization period. Both substrates were admitted to the vacuum chamber to nominally 2 to 5×10^{-6} torr through leak valves. Helium buffer gas was also admitted to 1 mtorr. The complex of interest was isolated by application of a combination of radio frequency and direct current voltages to the ring electrode (apex isolation mode [57]).

For CAD experiments in the triple quadrupole instrument, the hydrogen-bonded complex of interest was mass-selected with the first quadrupole, then accelerated into the collision quadrupole filled with argon. The kinetic energy of the ion was varied from 0 to 25 eV in the laboratory frame, which corresponded to approximately 0 to 3 eV relative kinetic energy (i.e., collision energy). The resulting fragment ions were mass analyzed in the third quadrupole. The constant precursor transmission mode was used, and the collision gas pressure was varied from 0.2 to 1.5 mtorr. The

signal-to-noise ratio for all spectra was typically at least 100:1. The absolute conversion efficiencies of precursor ions to fragment ions based on a comparison of the intensity of the precursor ion signal in the absence of target gas to the summed intensities of the fragment ions was 2% to 75% depending on the collision energy and pressure. Single collision conditions were estimated by the method of Bursey et al. [58] and Dawson et al. [59]. In all cases the results are tabulated as a function of laboratory kinetic energy. There are small variations (± 0.2 eV) in the resulting relative collision energies for complexes of different mass, with the complexes of lower mass having slightly higher kinetic energies. In fact, energy-resolved breakdown curves show that an extra 0.2 eV relative kinetic energy does not promote additional skeletal decomposition of the 12-crown-4 complexes (a representative system). Thus, in the context of this study, this energy variation is not expected to cause any qualitative discrepancy in the results. In the ITMS, CAD was performed by application of a 100 to 500 mV resonant voltage across the end-cap electrodes for 5 to 10 ms ($q = 0.4$).

All compounds except 21-crown-7 were obtained from Aldrich Chemical Co. (Milwaukee, WI) and used without further purification. The 21-crown-7 was obtained from Parish Chemical Co. (Orem, UT). Purities were > 97%.

Results and Discussion

The major objective of these studies is to develop a means of evaluating the differences in hydrogen-bonding interactions of polyether/ammonium ion complexes based on interpretation of many CAD experiments done to characterize the dissociation reactions of the complexes. Dissociation rate versus internal energy diagrams are useful for depicting the competing dissociation pathways of ions, trends which are reflected in the observed CAD patterns. If two competing dissociation pathways have similar transition state geometries (i.e., entropic requirements) but different activation energy barriers, then the abundances of the two fragment ions resulting from these two dissociation pathways will be proportional to the distribution of internal energies available to the precursor ions upon activation. If the two competing dissociation pathways have similar activation energy barriers but different transition state geometries such that one is a faster process, then the pathway of looser geometry will always lead to a more abundant fragment ion at all internal energies. In complex cases both the entropic factors and activation energies for competing processes will be different, and then the trends for dissociation may cross (Figure 1). For these latter situations, the relative abundances of fragment ions will vary with the internal energy available upon collisional activation of the precursor ion.

As shown in the next sections, the CAD experiments performed for elucidation of the model

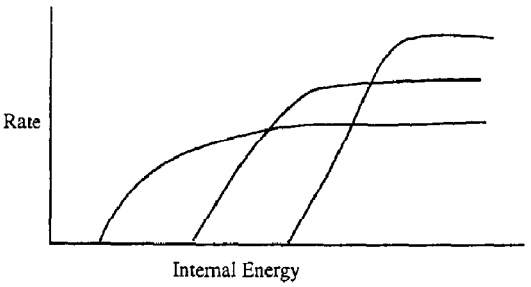

Figure 1. Kinetic trends for dissociation of ions having different activation energies and entropic factors. The trends represent complex dissociation reactions.

host–guest complexes in this study lead to several general types of fragmentation behavior which are interpreted in terms of the nature of binding interactions. The formation of only protonated polyether molecules and/or protonated amine molecules upon dissociation of a selected polyether/ammonium ion complex is presumed to indicate that the overall weakest bonding interactions in the ion complex are the hydrogen bonds involved in complexation, and the activation barrier to dissociation by decomplexation is lower than the various activation barriers for subsequent covalent bond cleavages within the polyether or amine. In contrast, the formation of fragment ions corresponding to covalent bond cleavages within the polyether portion of the ion complex is assumed to indicate that the total hydrogen-bonding association energy of the complex is sufficiently large to result in a relatively high activation barrier to dissociation. Presumably this activation barrier may be an energy barrier (i.e., from the multiple hydrogen bonds of the complex) or an entropy barrier (i.e., due to unfavorable configurational requirements because of the many active vibrational modes in the complex). In either case, surpassing this high barrier to decomposition can result in formation of internally excited protonated polyether molecules that may then undergo subsequent fragmentation by skeletal cleavages.

Potential energy diagrams which also may be used to rationalize these situations are shown in Figure 2. As illustrated in Figure 2 by the solid curve, both the activation barrier to decomplexation and the reverse activation energy for formation of the intact protonated polyether are large. Under these circumstances, the protonated ether resulting from decomplexation is internally excited and may undergo spontaneous dissociation by cleavages of the polyether skeleton, especially when the barriers to subsequent dissociation are relatively low (as is the case for protonated polyethers). As illustrated in Figure 2 by the dashed curve, if the barriers to dissociation are low, the polyether/ammonium ion complex simply decomplexes and subsequent disruption of the polyether skeleton will not be favored.

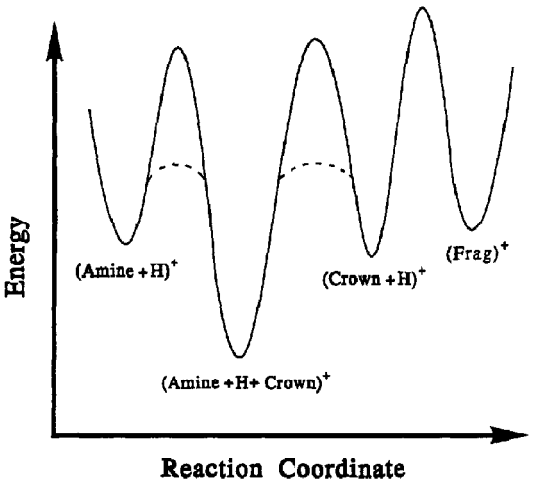

Figure 2. Proposed energy diagram for the dissociation of a polyether/ammonium ion complex. Dotted line represents a loosely bound complex, solid line represents a strongly bound complex.

In the context of this study, several types of CAD experiments assist in determining the nature of the hydrogen-bonding interactions of the complexes. First, one can examine energy-, time-, and pressure-resolved collisional activation data to monitor the effects of energy deposition and time scale of activation. Second, one can begin to evaluate the importance of entropy effects by varying the nature of the model amine guest (floppy versus small polyatomic versus bulky molecule) and the polyether host (flexible acyclic ether versus more rigid cyclic ether). In the latter case both glycols and glymes are acyclic analogs to the cyclic crown ethers, and thus they have similar types of vibrational modes involved in internal energy redistribution. Ultimately, in this systematic study the dissociation trends observed for the different polyether/amine complexes are interpreted as reflecting the nature of the hydrogen-bonding interactions involved in stabilizing the ions in the gas phase.

Collision-Activated Dissociation in the Triple Quadrupole Mass Spectrometer

The CAD results obtained by using a triple quadrupole mass spectrometer are summarized in Table 2. Examples of the strikingly distinctive types of dissociation behavior obtained for two different crown ether/amine ion complexes, 18-crown-6 and pyridine or 18-crown-6 and 2-aminoethanol, are shown in Figure 3. Because pyridine and 2-aminoethanol both have similar gas-phase basicities, 213.1 kcal/mol and 213.4 kcal/mol [60], respectively, they provide an interesting comparison of complex formation with 18-crown-6, whose gas-phase basicity is estimated as 216.0 kcal/mol [43]. Activation of the proton-bound 18-crown-6/2-aminoethanol ion complex results in extensive fragmentation of the crown ether ring (Figure 3b at 0.2 mtorr argon) by losses of ethylene oxide units. In contrast, collisional activation of the proton-bound 18-crown-6/pyridine ion complex results in formation of predominantly protonated pyridine and protonated 18-crown-6 (Figure 3a at 1.1 mtorr argon) with little fragmentation of the crown ether ring, even under a range of quite energetic conditions.

The dissociation trends illustrated in Figure 3a from the 18-crown-6/pyridine ion complex are characteristic of the general type of hydrogen-bonded complexes which simply disassemble after activation. These complexes are presumably weakly bound, with little evidence for substantial energy tied into the binding interactions. With respect to the specific case shown in Figure 3a, the fact that the abundance of protonated pyridine is greater than that of protonated 18-crown-6 is interesting because 18-crown-6 has a substantially higher gas-phase basicity, and one might expect it to

Table 2. Collision-activated dissociation of crown ether/amine ion complexes in a TSQ mass spectrometer[a]

Amine	12-Crown-4			15-Crown-5			18-Crown-6		
	$(AmH)^+$	$(CrH)^+$	$\Sigma Frgs^+$	$(AmH)^+$	$(CrH)^+$	$\Sigma Frgs^+$	$(AmH)^+$	$(CrH)^+$	$\Sigma Frgs^+$
Propylamine	85	15	0	10	65	25	5	25	70
2,5-Dimethylpyrrole	90	10	0	80	20	0	30	65	5
2-Chloro-6-methylpyridine	90	10	0	20	80	0	20	75	5
2-Methylaziridine	80	20	0	20	50	30	30	10	60
Pyridine	97	3	0	95	5	0	90	10	0
2-Aminoethanol	90	10	0	30	20	50	5	35	60
3-Aminopropanol	100	0	0	100	0	0	20	20	60
Diethylamine	100	0	0	100	0	0	100	0	0
3,5-Lutidine	100	0	0	100	0	0	100	0	0
Ethylene diamine	100	0	0	60	5	35	60	10	30
4-Aminobutanol	100	0	0	100	0	0	100	0	0
5-Aminopentanol	100	0	0	100	0	0	100	0	0

[a] $(AmH)^+$, $(CrH)^+$, and ΣFrg^+ represent the percentage ion current due to formation of the protonated amine, protonated crown ether, and the sum of the fragments from the crown ether (such as ions at m/z 89, 133, and 177), respectively. All values are ±5%, based on the average of day-to-day variations in CAD spectra at 15 eV, 0.7 mtorr argon.

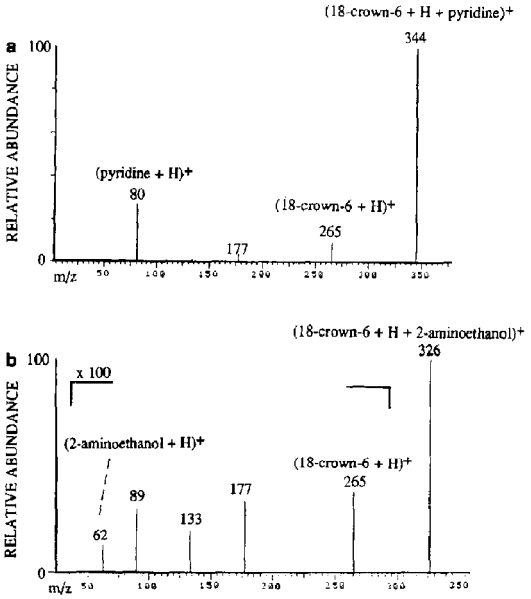

Figure 3. CAD spectra of **(a)** (18-crown-6 + H + pyridine)$^+$ complex at 1.1 mtorr collision pressure, and **(b)** (18-crown-6 + H + 2-aminoethanol)$^+$ complex at 0.2 mtorr collision pressure (collision energy was 5 eV in a triple quadrupole mass spectrometer). Different collision gas pressures were used to emphasize that the latter complexes fragment extensively even under single collision activation conditions, whereas the former do not show very much macrocyclic cleavage even under multiple collision conditions. The ions of m/z 89, 133, and 177 are crown-ether related fragment ions. All values are ±5%.

bind the proton more strongly in the proton-bound complex. However, the high gas-phase basicity of 18-crown-6 stems specifically from the fact that it may stabilize a proton through multiple hydrogen-bonding interactions (i.e., formation of a proton bridge between two oxygen atoms), whereas pyridine is recognized as a strong monodentate ligand [44, 45]. When the 18-crown-6 molecule is involved in formation of a proton-bound complex with pyridine, the usual multidentate proton-binding interactions are perturbed and a new proton bridge between an ether oxygen and the nitrogen of pyridine forms. Thus, when the complex disassembles, the pyridine moiety more effectively retains the proton.

Figure 3b shows the dissociation spectrum of the 18-crown-6/2-aminoethanol complex, one in which multiple hydrogen-bonding interactions between the two organic substrates apparently are significant. For example, the binding interactions may include coordination of two of the crown ether oxygens to two of the amine hydrogens, proton-bridge formation between one of the crown ether oxygens and the nitrogen atom, and one final hydrogen bond between an ether oxygen and the hydroxyl hydrogen of the aminoalcohol. In this case, simple decomplexation to form protonated 18-crown-6 and protonated 2-aminoethanol is not the most favored process. Instead, ions due to cleavages and rearrangements of covalent bonds in the crown ether skeleton are predominant, leading to formation of ions at m/z 89, 133, and 177. This behavior suggests that the interaction energy of the complex may be sufficiently high such that the energy necessary to surpass the dissociation threshold results in an internally hot macrocyclic ion which may then undergo further fragmentation.

Results of collisional activation experiments for other crown ether/amine complexes (Table 2) can be conveniently categorized based on the known thermochemical properties and structures of the participating molecules. For those crown ether/ammonium ion complexes in which the gas-phase basicity of the amine substrate is more than 3 kcal/mol greater than the basicity of the crown ether, then typically only the ammonium ion is formed after collisional activation (such as the 3-aminopropanol/12-crown-4, diethylamine/15-crown-5, and 4-aminobutanol/18-crown-6 ion complexes). Those complexes may be represented conceptually as ones bound by a "single" proton-bridge with the proton much more strongly coordinated to the amine (i.e., the formation of multiple hydrogen bonds is not indicated). This case is especially predominant for those complexes involving 12-crown-4, the macrocycle with the smallest cavity size, the lowest gas-phase basicity, the smallest number of hydrogen-bond accepting oxygen donors, and having the least favorable entropic factors for participating in multiple hydrogen bonds.

For the cases in which the gas-phase basicities of the two components involved in the complex differ by less than 3 kcal/mol and the number of possible hydrogen-bonding interactions is three or less, then typically a mixture of intact protonated crown ether molecules and ammonium ions is formed, but extensive fragmentation of the crown ether is not observed (such as the propylamine/12-crown-4, 2,5-dimethylpyrrole/15-crown-5, and pyridine/18-crown-6 ion complexes). Even under multiple collision activation conditions which favor stepwise activation and fragmentation, typically 95% of the dissociation products are intact ammonium or crown ether ions and less than 5% of the products are crown ether-related fragments. This case is energetically represented in Figure 2 with the activation barriers to decomplexation shown as dashed lines. Because the complex is weakly bound, the dissociation barriers are low and the amount of internal energy required to induce dissociation of the complex is less than that required to access skeletal cleavages of the macrocycle. In contrast to the first case described, in these complexes both the ether and the amine are somewhat equally coordinated to the proton, and thus both compete effectively for retention of the proton. Presumably, the kinetics of decomplexation are also fast due to the low number of binding interactions.

The final case is that in which extensive fragmenta-

tion of the polyether is observed (even after single collision activation), and this occurs for those complexes which generally can permit more than three favorable hydrogen-bonding interactions (i.e., the 2-aminoethanol/15-crown-5, and ethylene diamine/18-crown-6 ion complexes) or when the known gas-phase basicity of the polyether is greater than that of the amine (i.e., propylamine with 18-crown-6 or 15-crown-5). This general case represents strongly bound complexes whose dissociation characteristics are dependent on both the relative difference in the gas-phase basicities of the amine and ether and the number of potential interactions. For example, the larger crown ethers (15-crown-5, 18-crown-6) have somewhat more flexible structures that are better able to accommodate multiple hydrogen-bonding interactions with the amine substrates, especially the difunctional amines such as ethylene diamine and 2-aminoethanol. Considerable abundances of crown ether skeletal fragment ions result after activation of these complexes (see Table 2). The energy diagram already shown in Figure 2 by the solid line describes this situation. Furthermore, the large number of hydrogen-bonding interactions would tend to promote slower dissociation kinetics, thus allowing more effective competition from slower reactions, such as those involving macrocyclic skeletal rearrangement and cleavage.

In most cases, the 15-crown-5 and 18-crown-6 ethers demonstrate similar propensities for skeletal cleavage (i.e., those complexes involving propylamine, 2-methylaziridine, 2-aminoethanol, ethylene diamine). However, 18-crown-6 also undergoes extensive skeletal fragmentation when complexed with 3-aminopropanol, whereas the analogous 15-crown-5/3-aminopropanol complex disassembles exclusively to protonated 3-aminopropanol. This represents a clear example in which a relatively small structural difference in the polyether moiety has a tremendous impact on the dissociation of the complex. The gas-phase basicity of 3-aminopropanol is greater than either of these crown ethers; however, 18-crown-6 not only competes more effectively for the proton than 3-aminopropanol (i.e., net 80% of the fragment ion current is due to protonated 18-crown-6 related ions, and only 20% is attributed to protonated 3-aminopropanol), but also undergoes extensive skeletal fragmentation during the dissociation process. After surmounting the high activation barrier representative of a strongly bound complex, the 18-crown-6/3-aminopropanol complex apparently has acquired sufficient internal energy to also surpass the dissociation barriers leading to covalent cleavages of the macrocycle. The 18-crown-6 molecule has several more vibrational modes than 15-crown-5, ultimately resulting in a slower dissociation rate too.

Interestingly, the 18-crown-6/4-aminobutanol complex exhibits the same dissociation characteristics as the 15-crown-5/3-aminopropanol complex: generation of only the protonated aminoalcohol and no observed fragmentation of the macrocyclic structure nor retention of the proton by the crown ether. Upon first inspection one might have predicted the 18-crown-6/4-aminobutanol complex to have the slowest dissociation kinetics of all of the ones discussed in this section because of its large size and many active vibrational modes. Thus, one might likewise have expected it to promote the kinetically slow dissociation reactions characteristic of macrocyclic bond cleavages. Such a fragmentation pattern is not observed. Evidently, the hydrogen bonds between the 18-crown-6 molecule and the 4-aminobutanolium ion are sufficiently weak (due to the large discrepancies in the overall proton-binding affinity of 18-crown-6 relative to 4-aminobutanol) that a "strongly bound" complex is not formed; the complex simply disassembles upon activation. The most noteworthy point from this comparison is the demonstration that the kinetics of dissociation as reflected by the CAD patterns are not dictated alone by a mere statistical counting of vibrational degrees of freedom, and instead must reflect the total effective hydrogen-bonding interaction strength of the complex.

Pressure and Energy-Resolved Collisional Activation Studies in a Triple Quadrupole Instrument

To probe in greater detail some of the factors that influence the dissociation behavior of the complexes, both pressure-resolved and energy-resolved studies were performed. For the pressure-resolved studies, the argon target gas pressure in the collision quadrupole was varied from 0.2 mtorr to 1.5 mtorr. This range of pressure represented single to multiple collision conditions [58, 59], with conversion efficiencies (precursor ions to fragment ions) ranging from 1% to 75%. For the energy-resolved studies, the laboratory collision energy was raised from 2 eV to 25 eV at a constant argon target gas pressure to examine the effects of the collision energetics on the resulting dissociation trends.

The pressure-resolved breakdown curves for the complexes of 15-crown-5 with 2-methylaziridine or with 2,5-dimethylpyrrole are shown in Figures 4 and 5. As already indicated in Table 2, under standard activation conditions the 15-crown-5/2,5-dimethylpyrrole complexes do not dissociate to any appreciable extent by cleavages of the crown ether skeleton. This absence of skeletal fragmentation at lower collision pressures is also noted in the pressure-resolved curves shown in Figure 4. Only at the higher collision gas pressures which represent the case of multiple activation steps does protonated 15-crown-5 (m/z 221) fragment to any considerable amount. At the highest pressures, the increasing abundance of the 15-crown-5 related fragment ion (i.e., m/z 133) is likely due to subsequent collisional activation of the protonated 15-crown-5 ions after decomplexation as the ions travel through the pressurized collision quadrupole. This general behavior suggests that for these types of complexes, simple

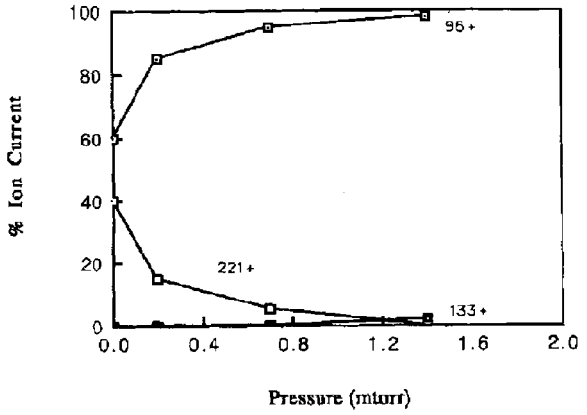

Figure 4. Pressure-resolved CAD breakdown curves for (5-crown-5 + H + 2,5-dimethylpyrrole)$^+$ complex (15 eV collision energy in a triple quadrupole mass spectrometer). The ion at m/z 133 is a crown ether fragment ion. All values are ±5%.

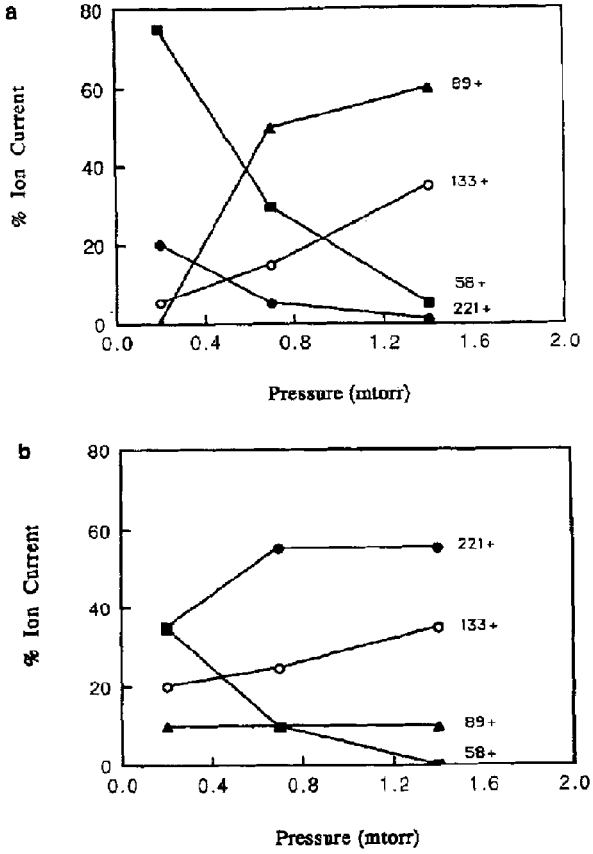

Figure 5. Pressure-resolved CAD breakdown curves for (15-crown-5 + H + 2-methylaziridine)$^+$ complex at (a) 15 eV collision energy and (b) 5 eV collision energy in a triple quadrupole mass spectrometer. Protonated 15-crown-5 appears at m/z 221. Protonated 2-methylaziridine appears at m/z 58. The ions of m/z 89, 133, and 177 are crown-ether related fragment ions. All values are ±5%.

decomplexation after collisional activation is most facile relative to the strength of the hydrogen bonds which stabilize the weakly bound complex.

In contrast, the 15-crown-5/2-methylaziridine complex shows extensive fragmentation of the macrocyclic structure under an array of different collisional activation conditions. At low pressures, protonated 2-methylaziridine is most abundant, and the abundance of protonated 15-crown-5 is only 20% of the ion current. Most interestingly, the total relative abundances of the crown ether fragment ions (m/z 133 and 89) increase dramatically with increasing collision gas pressure (Figure 5a). Because the sum of the abundances of all the fragment ions attributed to the crown ether versus the abundance of the 2-methylaziridinium ion increases at higher collision gas pressures, this suggests that the covalent cleavages within the crown ether portion of the complex become kinetically more competitive with stepwise activation. A likely rationalization is that the total internal energy deposition increases with the number of activation steps (i.e., collision gas pressure), so that new dissociation channels are accessible.

The energy-resolved breakdown curves shown in Figure 6 for dissociation of the 18-crown-6/2-aminoethanol complex are particularly revealing. The curves in Figure 6a represent single collision activation conditions, and the total relative abundance of all crown ether-related ions (m/z 89, 133, 177, and 265) decreases with increasing collision energy. These trends demonstrate that formation of protonated 18-crown-6 at m/z 265 by cleavage of the neutral amino alcohol and cleavages of the macrocyclic skeleton are all accessible at relatively low energy thresholds. Only at the higher collision energies can the complex dissociate alternately to the protonated amino alcohol, suggesting that it is a more endothermic process. These CAD patterns reflect the type of "dissociation rate versus internal energy" trends illustrated in Figure 1, sampling the lower energy portion of the curves.

Figure 6b shows the breakdown curves obtained under multiple collision conditions. Under these conditions the formation of the protonated amine (m/z 62) is never the most favored dissociation pathway, but again the trends for the relative abundances of product ions qualitatively duplicate those observed in Figure 6a: the abundance of m/z 265 (protonated 18-crown-6) decreases with increasing collision energy, the abundance of m/z 89 (crown ether fragment ion) increases with energy, and the abundance of m/z 62 (protonated 2-aminoethanol) increases slightly with energy. These trends indicate that the dissociation pathways leading to crown ether-related product ions have considerable activation barriers that are increasingly surmountable after stepwise energization (i.e., multiple collision conditions in which more energy can be accumulated than in the analogous single collision conditions described above), suggesting that the portion of the "dissociation rate versus internal energy" curves

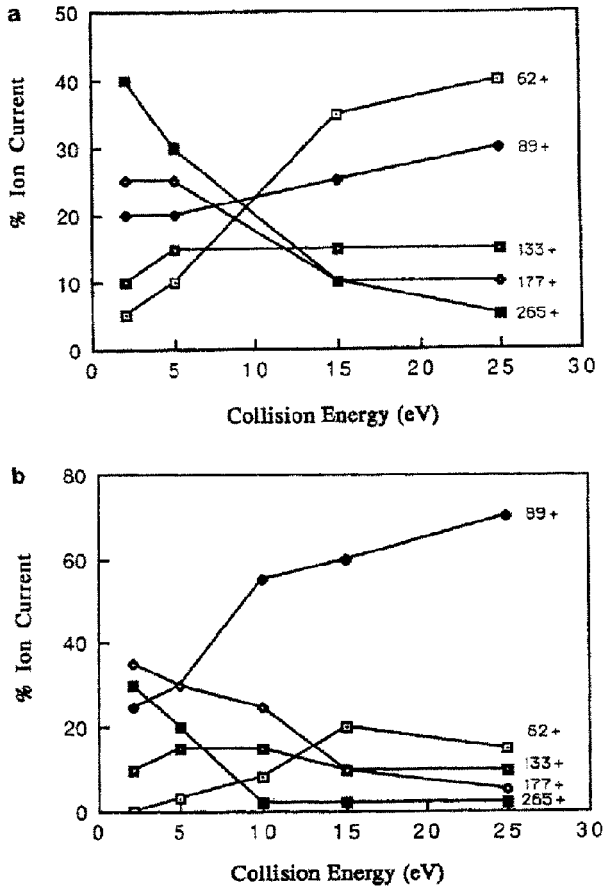

Figure 6. Energy-resolved CAD breakdown curves for (18-crown-6 + H + 2-aminoethanol)$^+$ complex at (a) 0.2 mtorr argon and (b) 1.0 mtorr argon in a triple quadrupole mass spectrometer. Protonated 2-aminoethanol appears at m/z 62. Protonated 18-crown-6 appears at m/z 265. The ions of m/z 89, 133, and 177 are crown-ether related fragment ions. All values are ±5%.

which is effectively sampled changes significantly upon switching from single-step to multi-step activation. Thus, in the latter case the entire trends depicted in Figure 1 may be operative, in which the third curve having the higher activation barrier cumulatively represents the various crown-ether related fragment ion pathways.

Collision-Activated Dissociation in a Quadrupole Ion Trap

Selected collisional activation experiments were done in a quadrupole ITMS to compare the dissociation behavior of crown ether/ammonium ion complexes formed and activated in a different environment than in the triple quadrupole instrument. In a quadrupole ion trap in which typically 1 mtorr of helium is present at all times, complexes are less efficiently deactivated as compared to deactivation in the relatively high pressure (2 torr methane) chemical ionization source of the triple quadrupole mass spectrometer. Thus, fewer loosely bound complexes survive in the quadrupole ion trap because the time scale for spontaneous dissociation competes on the time scale of collisional stabilization, and this is experimentally evident by the lower overall abundance of proton-bound complexes relative to the abundances of simple protonated crown ether and amine molecules formed during the ionization period. Moreover, collisional activation occurs in a stepwise manner in the quadrupole ion trap due to the high helium pressure and long activation time (5 to 10 ms) used. The fact that the ions are not accelerated to a high kinetic energy prior to collisions with helium but instead continuously undergo many collisions during excitation also causes different types of fragmentation processes to be favored. For example, those dissociation reactions that have low activation energies, such as is the case for many rearrangement processes, are especially favored [61]. Lastly, only those ions of a selected mass-to-charge ratio are resonantly activated in a quadrupole ion trap, and fragment ions formed during the CAD process are not activated further. This selectivity contrasts with activation in the triple quadrupole instrument because all fragment ions formed in the collision quadrupole may themselves undergo further activating collisions as they are accelerated out of the quadrupole.

A summary of the results for CAD of a series of amine/15-crown-5 ion complexes obtained with the quadrupole ITMS is shown in Table 3. For the ion complexes involving 15-crown-5 with 2-aminoethanol, pyridine or diethylamine, the CAD behavior in the ion trap is similar to that observed in the TSQ experiments. For example, extensive fragmentation of the crown ether is observed upon activation of the 2-aminoethanol/15-crown-5 complex, and predominantly dissociation to the protonated amine is observed after activation of the pyridine/15-crown-5 or diethylamine/15-crown-5 complexes. Additionally, activation of the ammonia/15-crown-5 ion complex in

Table 3. Collision-activated dissociation of 15-crown-5/amine ion complexes in a quadruple ITMS[a]

Amine substrate	$(AmH)^+$	$(CrH)^+$	$\Sigma Frgs^+$
Ammonia	nd[b]	55	45
Propylamine	88	4	8
2-Methyl-aziridine	90	10	0
Pyridine	95	4	1
2-Aminoethanol	30	20	50
Diethylamine	100	0	0
Ethylene diamine	100	0	0

[a] $(AmH)^+$, $(CrH)^+$, and ΣFrg^+ represent the percentage ion current due to formation of the protonated amine, protonated crown ether, and the sum of the fragments from the crown ether (such as ions at m/z 89, 133, and 177), respectively. All values are ±15%, based on the average of day-to-day variations in CAD spectra.

[b] The formation of NH_4^+ could not be detected in the ion trap because of the low-mass stability limit used for the CAD experiment.

the ion trap results in extensive fragmentation, an expected result based on the capability of ammonia to form multiple hydrogen bonds with 15-crown-5, thus creating a large activation barrier to dissociation.

There are also disparities between the CAD behavior of certain amine/15-crown-5 ion complexes observed in the quadrupole ion trap and triple quadrupole mass spectrometers. First, dissociation of the 2-methylaziridine/15-crown-5 complex is somewhat anomalous because fragmentation of the crown ether skeleton is not observed in the ion trap. However, this behavior does overlap with that observed from the TSQ experiments performed at lower collision gas pressure, 15 eV conditions (see Figure 5a). Second, activation of the propylamine/15-crown-5 complex in the ion trap results in formation of much more protonated propylamine than was observed in the triple quadrupole CAD spectra. Finally, the ethylenediamine/15-crown-5 complex dissociates very differently in the ion trap compared to the behavior observed in the triple quadrupole instrument. In the trap, the complex exclusively forms protonated ethylenediamine after activation—no protonated crown ether molecules or fragment ions are observed. In the triple quadrupole mass spectrometer, extensive fragmentation of the crown ether was observed. The results for these latter three crown ether/amine complexes suggest that perhaps the stepwise activation in the quadrupole ion trap occurs on a sufficiently slower time scale to prohibit increasing internal energy accumulation relative to competitive deactivation or dissociation processes. For instance, if each collision in the ion trap results in lower overall internal energy deposition than in the TSQ instrument, then it is possible that the activation barrier for dissociation to protonated 15-crown-5 is never surpassed on a time scale that competes with dissociation to the protonated amine through the lower activation energy pathway.

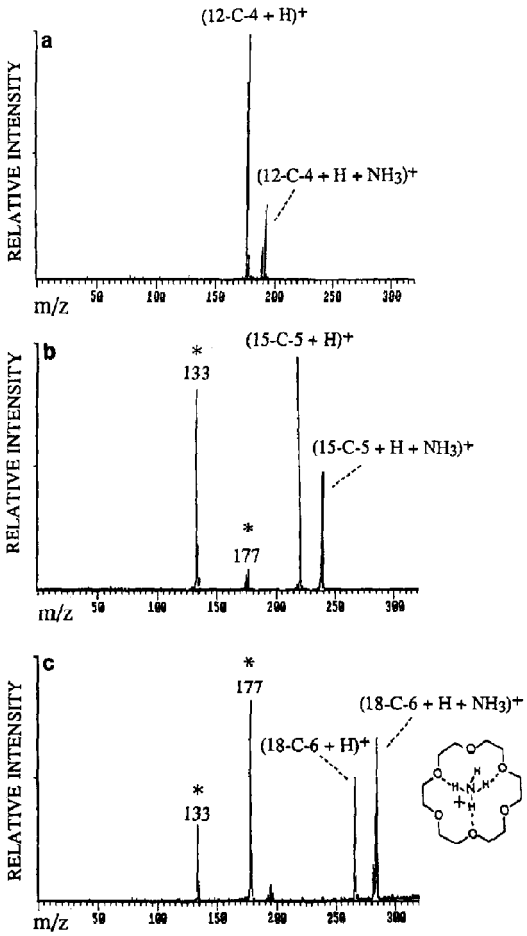

Figure 7. CAD spectra for the complexes (a) (12-crown-4 + H + NH_3)$^+$, (b) (15-crown-5 + H + NH_3)$^+$, and (c) (18-crown-6 + H + NH_3)$^+$ obtained in an ITMS (500 mV activation, q = 0.4). The peaks labeled with "*" are crown-ether fragment ions.

Polyether Size Effects on Complexation Interactions

A comparison of the dissociation patterns of complexes involving ammonia and three different crown ethers in the quadrupole ion trap proved particularly intriguing because ammonia is the smallest model guest and it may in fact bind within the cavity of the larger crown ethers. The systematic use of ammonia as the guest means that the active vibrational modes in the amine portion of the complex remain the same throughout this set of comparative experiments, and thus cannot contribute to qualitative variations in the results. Shown in Figure 7 are the CAD spectra for the complexes generated from reactions of ammonia with 12-crown-4, 15-crown-5, and 18-crown-6. In each case the ammonium ion complex was isolated and collisionally activated. The complex incorporating 12-crown-4 simply decomplexes after activation, and no skeletal fragmentation is observed (Figure 7a). In contrast, skeletal decomposition is observed for the complex involving the 15-crown-5 ligand (Figure 7b), and for the 18-crown-6 complex, the sum of the crown ether fragment ions is greater than the intensity of the intact protonated 18-crown-6. This striking variation in dissociation patterns supports an argument in which the strength of the collective hydrogen-bonding interactions of the complexes increases with the size of the crown ether and thus alters the resulting fragmentation patterns. Additionally, it should be noted that the number of internal vibrational modes of the polyether increases from 12-crown-4 to 15-crown-5 to 18-crown-6, presumably influencing the dissociation rates of the complexes. The overall slower decomposition rates of the complexes containing the larger crown ethers may allow increasing competition from pathways which involve macrocyclic bond cleavages.

However, it should be reemphasized that a cursory accounting of the individual vibrational modes of the

polyether and amine in a complex cannot be used to directly predict the extent of macrocyclic skeletal cleavage. If this simplified correlation were true, then the 18-crown-6/pyridine ion complex would be expected to undergo more extensive macrocyclic fragmentation than the 18-crown-6/ammonium ion complex. However, as evidenced in Tables 2, 3, and 4, this correlation is clearly not the case. One cannot simply state that the bigger, bulkier complexes dissociate slower and thus are more likely to undergo macrocyclic skeletal cleavage. Macrocyclic skeletal cleavage is only consistently observed when numerous hydrogen-bonding interactions are expected to be operative, regardless of the size or number of vibrational modes of the amine or polyether moiety.

Comparison of Complexes Involving Cyclic Versus Acyclic Polyether Ligands

To further evaluate the significance of entropic effects in influencing the energetics and/or kinetics of the dissociation pathways, the CAD spectra of complexes incorporating acyclic polyether ligands such as glymes and glycols were compared to the spectra described for the complexes involving cyclic ethers. Complexes involving three amine guests, pyridine, ammonia, and 2-aminoethanol, and nine acyclic ethers including ethylene glycol, diethylene glycol, triethylene glycol, tetraethylene glycol, pentaethylene glycol, ethylene glycol dimethyl ether, diethylene glycol dimethyl ether, triethylene glycol dimethyl ether, and tetraethylene glycol dimethyl ether were examined. In terms of model hosts the acyclic polyether ligands have similar numbers and types of vibrational modes compared to their crown ether counterparts and thus are relevant models to assist in probing the importance of the flexibility of the host structure on the dissociation behavior of the complexes. With respect to model guests, pyridine was selected because it represents a bulky guest with less propensity for multiple binding, whereas ammonia and 2-aminoethanol are amines that encourage multiple hydrogen-bonding interactions. Additionally, 2-aminoethanol is a more flexible model guest than pyridine or ammonia.

Each polyether/ammonium ion complex was formed in the quadrupole ion trap, then subjected to collisional activation. The CAD spectra for these complexes are summarized in Table 4. In some cases involving ethylene glycol or ethylene glycol dimethyl ether, the polyether/ammonium ion complex of interest was not successfully formed in the ion trap, presumably because the association reaction was too exothermic to permit effective stabilization of the resulting complex on the time scale of ion storage.

For all of the acyclic polyether/pyridinium ion complexes, dissociation results predominantly in decomplexation, forming protonated pyridine and protonated ether molecules. Fragmentation of the acyclic ether is never significant, regardless of the size or basicity of the polyether. This reaffirmed that the formation of multiple hydrogen bonds is not indicated for these complexes, just as noted for the crown ether/pyridinium ion complexes. For the complexes involving the larger crown ethers (21-crown-7, 18-crown-6), some macrocyclic skeletal fragmentation is observed, and the relative extent increases with the size of the ether.

In contrast, dissociation of many of the ammonium and 2-aminoethanol ion complexes results in extensive fragmentation of the ether ligands, especially for the larger crown ethers and glymes. The extent of ether skeletal cleavage increases with the number of oxygen binding sites of the ether. This latter result suggests that the number of possible hydrogen-bond acceptor

Table 4. Distribution of fragment ion current from CAD of acyclic and cyclic polyether ammonium ion complexes

	NH_3		Pyridine			2-Aminoethanol		
	$(M+H)^+$	$\Sigma Frgs^+$	$(Pyr+H)^+$	$(M+H)^+$	$\Sigma Frgs^+$	$(2\text{-}AE+H)^+$	$(M+H)^+$	$\Sigma Frgs^+$
Glyme	X[b]	X	100	0	0	X	X	X
Diglyme	85	15	100	0	0	100	0	0
Triglyme	60	40	100	0	0	95	4	1
Tetraglyme	45	55	95	5	0	40	30	30
Glycol	X	X	X	X	X	X	X	X
Diglycol	98	2	100	0	0	X	X	X
Triglycol	90	10	100	0	0	100	0	0
Tetraglycol	75	25	5	95	0	1	69	30
12-Crown-4	> 95	< 5	100	0	0	45	50	5
15-Crown-5	55	45	96	4	1	30	20	50
18-Crown-6	30	70	80	16	4	20	10	70
21-Crown-7	5	95	40	40	20	X	X	X

[a] $(M+H)^+$ represents the protonated polyether, $(2\text{-}AE+H)^+$ represents protonated 2-aminoethanol, and $(Pyr+H)^+$ represents protonated pyridine. $\Sigma Frgs^+$ represents the sum of all the polyether-related fragment ions.

[b] X indicates that the complex was not successfully formed, so the CAD experiment could not be performed.

sites influences the interaction energy in a way similar to the trend noted previously for the crown ethers. Also, the observation of extensive fragmentation of the acyclic ether ligands, just as was observed for the complexes involving cyclic ethers, supports the idea that the flexible acyclic ligands may participate in the types of multiple bonding interactions already described for the preorganized crown ethers.

However and most interestingly, some of the crown ethers show less extensive fragmentation overall than their acyclic counterparts. For example, the ammonium ion complex involving tetraglyme shows an abundance ratio for $(M + H)^+$: Σ (fragment ions) equal to 4:5, whereas the ratio is only 5:4 for 15-crown-5 and 7:3 for tetraglycol. The hydrogen bonds in the tetraglyme complex may be collectively more favorable than those in the 15-crown-5 complex because tetraglyme is a more flexible ligand which can wrap around ammonia, whereas ammonia is too large to fit in the cavity of 15-crown-5. Also, the kinetics for dissociation may be sufficiently slower for the floppy acyclic ligands, permitting greater competition from slower dissociation pathways. In either case, this result demonstrates that the cyclic ethers have qualitatively similar but quantitatively different binding natures than the acyclic ligands.

In general, the glycols show the lowest extent of skeletal cleavage. This result may be related to the fact that glycols have terminal hydroxyl groups which participate in different types and/or strengths of hydrogen bonds than do ether functional groups, thus altering the dissociation dynamics of the complexes. Clearly, the fact that glycols do not exhibit the same extent of skeletal fragmentation as either the crown ethers or glymes indicates that kinetics alone cannot explain the differences in fragmentation patterns because the glycols are also floppy ligands which would be expected to promote slower dissociation kinetics (and thus a corresponding increase in skeletal decomposition).

Interestingly, for the dissociation of the $(M + NH_4)^+$ complexes, the extent of polyether skeletal fragmentation increases with the relative order of ammonium ion affinities of the polyethers, which have been reported previously [49]. This correlation supports the idea that the interaction energy of the complex influences the dissociation of the ion in a predictable fashion that is directly related to the thermochemical properties of each polyether ligand.

Energy-Resolved and Time-Resolved Collisional Activation in a Quadrupole Ion Trap

The effects of activation time and voltage on the resulting CAD spectra of several crown ether complexes in the quadrupole ion trap were evaluated to obtain additional information about the nature of the complexes. In general, as the amplitude of the activation voltage or time used to excite a complex in the ion trap is increased, two changes are observed in the resulting CAD spectra: the total number of complexes that dissociate increases, and the average internal energy deposition increases so that higher energy dissociation pathways are accessed. Two points were of considerable interest for this study. First, comparison of the relative appearance thresholds for the decomplexation process and the fragment ions may reveal whether there is a significant difference in the energy needed to promote decomplexation versus skeletal fragmentation. Such a result would potentially allow distinction between the activation barrier height for decomplexation relative to the barrier height for skeletal fragmentation. Second, observation of variations in the relative abundances of the fragment ions may assist in determining whether entropic or energetic factors influence the dissociation behavior of the complexes. The dissociation behavior of the complexes involving ammonia or 2-aminoethanol were studied in greatest detail because activation of these complexes resulted in the largest extent of cleavage of the polyether skeleton.

Two representative energy-resolved breakdown curves for ammonium ion complexes of diglyme, $(M + H + NH_3)^+$ and (15-crown-5 + H + 2-aminoethanol)$^+$, are shown in Figures 8 and 9, respectively. In Figure 8, the ions at m/z 103 and 59 are typical fragment ions from protonated diglyme, formed by elimination of H_2O and $(H_2O + C_2H_4O)$, respectively. In Figure 9, the ion at m/z 133 is a well-known fragment ion of protonated 15-crown-5. In each case the threshold for decomplexation and the threshold for dissociation to form polyether fragment ions are identical within experimental error. This result demonstrates that there is a barrier which prevents the ammonium ion complexes from dissociating until there is substantial energy accumulation in the complex. The energy-resolved mass spectrometry (ERMS) trends observed in Figures 8 and 9 qualitatively resemble the type of ERMS trends obtained for the other polyether/ammonium ion complexes in the ion trap. However, for some of the complexes involving 18-crown-6, 15-crown-5, triethylene glycol, and tetraethy-

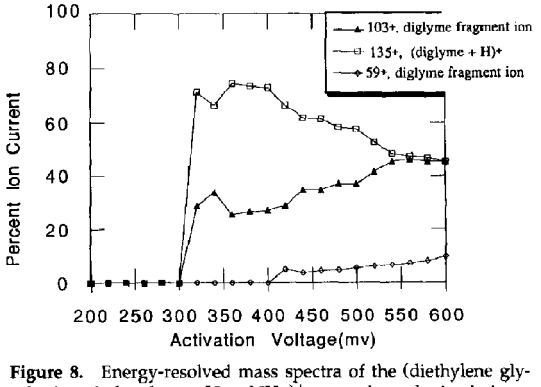

Figure 8. Energy-resolved mass spectra of the (diethylene glycol dimethyl ether + H + NH_3)$^+$ complex obtained in a quadrupole ITMS. All values are ±10%.

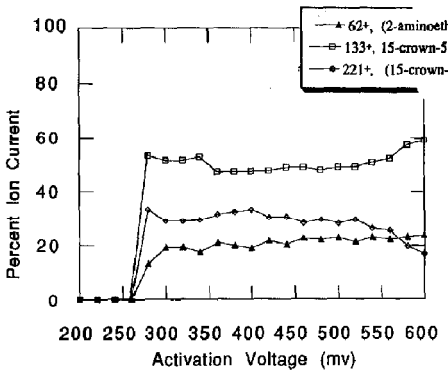

Figure 9. The energy-resolved mass spectra of the (15-crown-5 + H + 2-aminoethanol)$^+$ complex obtained in a quadrupole ITMS. All values are ±10%.

lene glycol with NH_3 or 2-aminoethanol ions, there is a small off-set between the threshold for decomplexation and the threshold for skeletal fragmentation. The thresholds for decomplexation and macrocyclic skeletal cleavage are close to each other (within 20 mV activation voltage). This offset suggests that the barrier height for skeletal cleavage may indeed be slightly higher than the one for decomplexation, but it also supports the idea that the complex is substantially internally excited prior to decomplexation.

For the time-resolved studies, each complex formed between a polyether and amine was isolated, then activated from 2 to 10 ms. One example representative of the type of time-dependent dissociation trends observed is shown in Figure 10 for the 15-crown-5/ammonium ion complex. There are no measurable changes in the abundances of the fragments relative to the abundances of the intact protonated ether molecules.

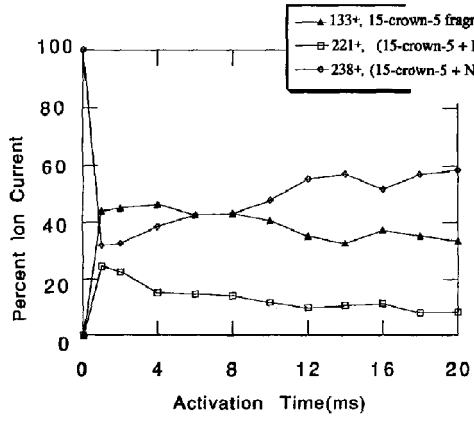

Figure 10. The time-resolved spectra of (15-crown-5 + H + NH_3)$^+$ complex obtained in a quadrupole ITMS. All values are ±10%.

This result shows that a longer activation interval does not significantly enhance the formation of any particular type of fragment ion.

Thermochemistry of Dissociation Reactions

Finally, the thermochemistry of the dissociation reactions of protonated crown ethers was estimated to obtain an understanding of the energetics of fragmentation of protonated macrocycles. The energy required for formation of each possible protonated cyclic ether and neutral cyclic ether counterpart from cleavage of the selected protonated crown ether was calculated from known heats of formation of the products and reactants [60, 62] (see Table 5). Each of the dissociation reactions examined are 14 to 35 kcal/mol endothermic, and these values set the lower bounds on the extra energy required by any protonated crown ether to promote dissociation. Additional energy may be required to surmount other activation barriers, and entropic barriers may also exist. However, as a first-order estimation of the energetics involved in dissociation of the crown ether/amine complexes, these numbers suggest that some of the complexes must be bound by at least 14 to 35 kcal/mol for the subsequent crown ether cleavages to occur.

Conclusions

The formation of multiple hydrogen bonds can have striking effects on the dissociation behavior of polyether/ammonium ion complexes because the multiple hydrogen-bonding interactions allow formation of strongly bound complexes in contrast to the loosely bound proton-bridged complexes that are typically formed by ion–molecule association reactions. The extent of polyether skeletal cleavage can thus be correlated with the collective hydrogen-bonding interactions of the complex. Both the number of possible interactions and thermodynamic factors affect the capability of any polyether and amine for forming a strongly bound complex. The ability to form multiple bonds can compensate for a relatively large difference in intrinsic proton binding affinity, but ultimately a very large difference in gas-phase basicity causes one substrate to be much more strongly coordinated to the proton, resulting in a less stable complex. These studies have provided insight into some of the requirements for multiple binding interactions of simple model host–guest systems in the gas phase and have shown that the occurrence of such multiple binding interactions can be evaluated experimentally by application of CAD techniques. Moreover, the results of this study have illustrated that model host–guest complexes formed in the gas phase may demonstrate binding properties that parallel the types of multiple interactions that govern complexation in solution.

Table 5. Thermochemistry of dissociation reactions of protonated crown ethers[a]

		Products				
Crown ether	ΔH_f	Ion	ΔH_f	Neutral	ΔH_f	ΔH_{rxn}
$(12-C-4+H)^+$	−7	$C_6H_{13}O_3^+$ (*m/z* 133)	40	C_2H_4O	−12.6	34.4
$(12-C-4+H)^+$ (*m/z* 177)	−7	$C_4H_9O_2^+$ (*m/z* 89)	96	$C_4H_8O_2$	−70	33
$(15-C-5+H)^+$	−49	$(12-C-4+H)^+$ (*m/z* 177)	−7	C_2H_4O	−12.6	29.4
$(15-C-5+H)^+$	−49	$C_6H_{13}O_3^+$ (*m/z* 133)	40	$C_4H_8O_2$	−70	19
$(15-C-5+H)^+$ (*m/z* 221)	−49	$C_4H_9O_2^+$ (*m/z* 89)	96	$C_6H_{12}O_3$	−110	35
$(18-C-6+H)^+$	−91	$(15-C-5+H)^+$ (*m/z* 221)	−49	C_2H_4O	−12.6	29.4
$(18-C-6+H)^+$	−91	$(12-C-4+H)^+$ (*m/z* 177)	−7	$C_4H_8O_2$	−70	14
$(18-C-6+H)^+$	−91	$C_6H_{13}O_3^+$ (*m/z* 133)	40	$C_6H_{12}O_3$	−110	21
(*m/z* 265)	−91	$C_4H_9O_2^+$ (*m/z* 89)	96	$C_8H_{16}O_4$	−151	36

[a] All values obtained or estimated from ref 60, in kilocalories per molecule.

Acknowledgments

The support from the Welch Foundation (F-1155), NIH (RO1 GM46723-01), and an ACS-PRF grant (22270-G5) are acknowledged.

References

1. Rebek, Jr., J.; Askew, R.; Ballester, P.; Costero, A. *J. Am. Chem. Soc.* **1986**, *110*, 923.
2. Etter, M. C., *Acc. Chem. Res.* **1990**, *23*, 120.
3. Vinogradov, S. N.; Linnel, R. H. *Hydrogen Bonding*. Van Nostrand Reinhold: New York, 1971.
4. Capon, B.; McManus, S. P. *Neighboring Group Participation*, vol. 1; Plenum Press: New York, 1976.
5. Caffrey, M. S.; Daldal, F.; Holden, H. M.; Cusanovish, M. A. *Biochemistry* **1991**, *30*, 4119.
6. Jeffrey, G. A.; Maluszynska, H. *Int. J. Quantum Chem.* **1981**, *8*, 231.
7. Santa Lucia, J.; Kierzek, R.; Turner, D. H. *Biochemistry* **1991**, *30*, 8242.
8. Cram, D. *Science* **1988**, *240*, 760.
9. Lehn, J. M. *Angew. Chem. Int. Ed. Engl.* **1988**, *27*, 89.
10. Sutherland, I. *Chem. Soc. Rev.* **1986**, *15*, 63.
11. Vogtle, F.; Weber, E., Eds. *Host Guest Complex Chemistry: Macrocycles*. Springer-Verlag: New York, 1985.
12. Takeda, Y. *Top. Curr. Chem.* **1984**, *121*, 1.
13. Weber, E.; Vogtle, F. *Top. Curr. Chem.* **1981**, *98*, 1.
14. Cram, D. J.; Trueblood, K. N. *Top. Curr. Chem.* **1981**, *98*, 43.
15. Izatt, R. M.; Eatough, D. J.; Christensen, J. J. *Struct. Bonding* **1973**, *16*, 161.
16. Mallinson, P. R.; Truter, M. R. *J. Chem. Soc. Perkin Trans. II* **1972**, 1818.
17. Vogtle, F.; Weber, E. In *The Chemistry of the Ether Linkage, Supplement E*; S. Patai, Ed. Wiley: London, 1981; p 59.
18. Lehn, J. M. *Struct. Bonding* **1973**, *16*, 1.
19. Izatt, R. M.; Terry, R. E.; Haymore, B. L.; Hansen, L. D.; Dalley, N. K.; Avondet, A. G.; Christensen, J. J. *J. Am. Chem. Soc.* **1976**, *98*, 7620.
20. Izatt, R. M.; Bradshaw, J. S.; Nielson, S. A.; Lamb, J. D.; Christensen, J. J.; Sen, D. *Chem. Rev.* **1985**, *85*, 271.
21. Wong, K. H.; Konizer, G.; Smid, J. *J. Am. Chem. Soc.* **1970**, *92*, 666.
22. Buschmann, H.-J. *J. Soln. Chem.* **1987**, *16*, 181.
23. Mosier-Boss, P. A.; Popov, A. I. *J. Am. Chem. Soc.* **1985**, *107*, 6168.
24. Michaux, G.; Reisse, J. *J. Am. Chem. Soc.* **1982**, *104*, 6895.
25. Frensdorff, H. K. *J. Am. Chem. Soc.* **1971**, *93*, 600.
26. Arnett, E. M.; Moriarity, T. C. *J. Am. Chem. Soc.* **1971**, *93*, 4908.
27. Lehn, J. M. *Angew. Chem.* **1988**, *27*, 89.
28. Hori, K.; Yamada, H.; Yamabe, T. *Tetrahedron* **1983**, *19*, 67.
29. Live, D.; Chan, S. I. *J. Am. Chem. Soc.* **1976**, *98*, 3769.
30. Dunitz, D. J.; Seiler, P. *Acta. Cryst. B.* **1974**, *30*, 2739.
31. Wipff, G.; Weiner, P.; Kollman, P. *J. Am. Chem. Soc.* **1982**, *104*, 3249.
32. Drew, M. G. B.; Yates, P. C. *Pure and Appl. Chem.* **1989**, *61*, 835.
33. Mazor, M. H.; McCammon, J. A.; Lybrand, T. P. *J. Am. Chem. Soc.* **1990**, *112*, 4411.
34. Cabbiness, D. K.; Margerum, D. W. *J. Am. Chem. Soc.* **1969**, *91*, 6540.
35. Hancock, R. D.; McDougall, G. J. *J. Am. Chem. Soc.* **1980**, *102*, 6551.
36. Sieger, H.; Vogtle, F. *Angew. Chem. Int. Ed. Engl.* **1978**, 17, 198.
37. Vogtle, F.; Weber, E. *Angew. Chem. Int. Ed. Engl.* **1979**, *18*, 753.
38. Johnstone, R. A. W.; Lewis, I. A. S. *Int. J. Mass Spectrom. Ion Phys.* **1983**, *46*, 451.
39. Bonas, G.; Bosso, C.; Vignon, M. R. *J. Incl. Phen. Mol. Recogn. in Chem.* **1989**, *7*, 637.
40. Morton, T.; Beauchamp, J. *J. Am. Chem. Soc.* **1972**, *94*, 3671.
41. Aue, D.; Webb, H.; Bowers, M. *J. Am. Chem. Soc.* **1973**, *95*, 2699.
42. Liou, C.-C.; Eichmann, E.; Brodbelt, J. S. *Org. Mass Spectrom.* **1992**, *27*, 1098.
43. Sharma, R. B.; Blades, A. T.; Kebarle, P. *J. Am. Chem. Soc.* **1984**, *106*, 510–516.
44. Meot-Ner, M. *J. Am. Chem. Soc.* **1983**, *105*, 4906–4911.
45. Meot-Ner, M. *J. Am. Chem. Soc.* **1983**, *105*, 4912–4915.
46. Brodbelt, J.; Maleknia, S.; Liou, C.; Lagow, R. *J. Am. Chem. Soc.* **1991**, *113*, 5913–5914.
47. Maleknia, S.; Brodbelt, J. *J. Am. Chem. Soc.* **1992**, *114*, 4295.
48. Liou, C.-C.; Brodbelt, J. *J. Am. Soc. Mass Spectrom.* **1992**, 3, 543.
49. Liou, C.-C.; Brodbelt, J. *J. Am. Chem. Soc.* **1992**, *114*, 6761.
50. Brodbelt, J.; Maleknia, S.; Lagow, R.; Lin, T. Y. *J. Chem. Soc., Chem. Commun.* **1991**, 23, 1705.
51. Maleknia, S.; Liou, C.-C.; Brodbelt, J. *Org. Mass Spectrom.* **1991**, *26*, 997.

52. Cooks, R. G.; Kruger, T. L. *J. Am. Chem. Soc.* **1977**, *99*, 1279–1281.
53. McLuckey, S. A.; Cameron, D.; Cooks, R. G. *J. Am. Chem. Soc.* **1981**, *103*, 1313–1317.
54. Zhang, H.; Chu, I.; Leming, S.; Dearden, D. A. *J. Am. Chem. Soc.* **1991**, *113*, 7415–7417.
55. Katritsky, A. R.; Malhotra, N.; Ramanathan, R.; Kemerait, R. C.; Zimmerman, J. A.; Eyler, J. R. *Rapid Commun. Mass Spectrom.* **1992**, *6*, 25.
56. Chu, I. H.; Zhang, H.; Deardon, D. V. *J. Am. Chem. Soc.* **1993**, *115*, 5736.
57. Weber-Grabau, M.; Kelley, P. E.; Syka, J. E. P.; Bradshaw, S. C.; Brodbelt, J. S. *Proceedings of the 35th Annual Conference American Society for Mass Spectrometry*; Denver, CO, 1987; p 1114.
58. Bursey, M. M.; Nystrom, J. A.; Hass, J. R. *Int. J. Mass Spectrom. Ion Processes* **1983**, *55*, 263.
59. Dawson, P. H.; French, J. B.; Buckley, J. A.; Douglas, D. J.; Simmons, D. *Org. Mass Spectrom.* **1982**, *17*, 205.
60. Lias, S. G.; Bartmess, J. E.; Liebman, J. F.; Holmes, J. L.; Levin, R. D.; Mallard, W. G. *J. Phys. Chem. Ref. Data* **1988**, *17*, suppl. 1.
61. Brodbelt, J. S.; Kenttamaa, H. I.; Cooks, R. G. *Org. Mass Spectrom.* **1988**, *23*, 6.
62. Lias, S. G.; Liebman, J. F.; Levin, R. D. *J. Phys. Chem. Ref. Data* **1984**, *13*, 695.